Biology of Reproduction, 2017, 96(2), 478–490
doi:doi:10.1095/biolreprod.116.143818
Research Article
Advance Access Publication Date: 11 January 2017

Research Article

Progressive obesity alters ovarian insulin, phosphatidylinositol-3 kinase, and chemical metabolism signaling pathways and potentiates ovotoxicity induced by phosphoramide mustard in mice†

Jackson Nteeba, Shanthi Ganesan, Jill A. Madden, Mackenzie J. Dickson and Aileen F. Keating*

Department of Animal Science, Iowa State University, Ames, Iowa, USA

*Correspondence: 2356J Kildee Hall, Department of Animal Science, Iowa State University, Ames, IA 50011, USA. Tel: +515-294-3849; Fax: +515-294-4471; E-mail: akeating@iastate.edu

†**Grant support**: The project described was partially supported by award number R00ES016818 to AFK. The content is solely the responsibility of the authors and does not necessarily represent the official views of the National Institute of Environmental Health Sciences or the National Institutes of Health.

Received 29 July 2016; Revised 2 December 2016; Accepted 21 December 2016

Abstract

Mechanisms underlying obesity-associated reproductive impairment are ill defined. Hyperinsulinemia is a metabolic perturbation often observed in obese subjects. Insulin activates phosphatidylinositol 3-kinase (PI3K) signaling, which regulates ovarian folliculogenesis, steroidogenesis, and xenobiotic metabolism. The impact of progressive obesity on ovarian genes encoding mRNA involved in insulin-mediated PI3K signaling and xenobiotic biotransformation [insulin receptor (*Insr*), insulin receptor substrate 1 (*Irs1*), 2 (*Irs2*), and 3 (*Irs3*); kit ligand (*Kitlg*), stem cell growth factor receptor (*Kit*), protein kinase B (AKT) alpha (*Akt1*), beta (*Akt2*), forkhead transcription factor (FOXO) subfamily 1 (*Foxo1*), and subfamily 3 (*Foxo3a*), microsomal epoxide hydrolase (*Ephx1*), cytochrome P450 family 2, subfamily E, polypeptide 1 (*Cyp2e1*), glutathione *S*-transferase (GST) class Pi (*Gstp1*) and class mu 1 (*Gstm1*)] was determined in normal wild-type nonagouti (a/a; lean) and lethal yellow mice (KK.CG-$A^{y/}$J; obese) at 6, 12, 18, or 24 weeks of age. At 6 weeks, ovaries from obese mice had increased ($P < 0.05$) *Insr* and *Irs3* but decreased ($P < 0.05$) *Kitlg*, *Foxo1,* and *Cyp2e1* mRNA levels. Interestingly, at 12 weeks, an increase ($P < 0.05$) in *Kitlg* and *Kit* mRNA, $pIRS1^{Ser302}$, $pAKT^{Thr308}$, EPHX1, and GSTP1 protein level was observed due to obesity, while *Cyp2e1* mRNA and protein were reduced. A phosphoramide mustard (PM) challenge increased ($P < 0.05$) ovarian EPHX1 protein abundance in lean but not obese females. In addition, lung tissue from PM-exposed animals had increased ($P < 0.05$) EPHX1 protein with no impact of obesity thereon. Taken together, progressive obesity affected ovarian signaling pathways potentially involved in obesity-associated reproductive disorders.

Summary Sentence

Obesity alters ovarian signaling pathways that regulate primordial follicle activation and chemical biotransformation, thereby potentially contributing to reproductive dysfunction.

Key words: ovary, obesity, phosphatidylinositol-3 kinase, ovotoxicant.

Introduction

The adverse effects of obesity on reproductive health have been documented, and include reduced conception and implantation [1, 2], impaired fecundity [2–5], increased infertility [1, 6], and an increase in offspring birth defects [7–9]. Obesity affects approximately 30% of US adults, with higher levels observed in African American (~48%) and Hispanic (~43%) populations [10]. The same pattern is true in children, with approximately 17% being obese, and there are differential obesity rates in African American (~20%) and Hispanic (~22%) children. Thus, obesity affects all communities, but some are more affected than others. The adverse effects of obesity on reproductive health have been documented, and include reduced conception and implantation [29, 30], impaired fecundity [30–33], and infertility [29, 34]. Obese mothers have increased risk for miscarriage [35], poor oocyte quality [36], and birth defects in their offspring [35]. It is also recognized that increased body mass index is a risk factor for many cancers, including ovarian cancer [37]. Mortality rates from ovarian cancer are greater in overweight and obese, relative to lean, women [38] and are also higher in African American relative to Caucasian women [39]. Furthermore, although studies are limited, a recent report positively associated human offspring cancer incidence with maternal obesity [40].

The mammalian ovary is the female gonad responsible for oocyte and steroid hormone production. At birth, a finite number of primordial follicles are present, arrested in the diplotene stage of prophase 1 [11]. Once primordial follicles are depleted, the female enters into ovarian senescence. A number of chemical exposures can result in follicle depletion leading to early ovarian senescence [12–16]. In addition, DNA damage [17] and altered folliculogenesis [18] due to ovotoxicant exposure have been reported. The ovary has the capacity to respond to such exposures through increased abundance of proteins involved in chemical biotransformation, including cytochrome P450 isoform 2E1 (*Cyp2e1*) [19–21], microsomal epoxide hydrolase (*Ephx1*) [22, 23], glutathione *S*-transferase Pi (*Gstp1*) [15, 24], and glutathione *S*-transferase Mu 1 (*Gstm1*) [25]. These enzymes are principally involved in the detoxification of xenobiotic compounds; however, their expression may also lead to bioactivation of some environmental compounds [12, 13, 19, 20, 26, 27].

The phosphatidylinositol-3 kinase (PI3K) signaling pathway plays a pivotal role in regulating ovarian folliculogenesis [28–31] and steroidogenesis [32–35]. We [36] and others [37–40] have demonstrated that obesity alters insulin-mediated signaling pathways, including PI3K. In addition, we have determined that PI3K signaling regulates abundance of the xenobiotic metabolism enzymes *Gstp1*, *Gstm1*, *Ephx1*, and *Cyp2e1* [18, 41–43]. Altered expression of genes involved in these pathways could sabotage proper ovarian function and consequently lead to impaired fertility. Adverse reproductive outcomes including anovulation, impaired fecundity, and premature ovarian failure can result from unregulated folliculogenesis. In the absence of ovarian function, females have a greater risk for development of gynecological cancers, osteoporosis, and cardiovascular disease [16, 27, 44]. We have demonstrated that obese female mice have reduced numbers of preantral follicles, relative to their lean counterparts [45]; however, the mechanisms involved remain unclear.

Despite a strong positive correlation between obesity and impaired reproductive capacity, the underlying mechanisms have not been clearly defined. To understand the onset and duration of changes in PI3K and chemical metabolism gene during obesity, we designed a study using the agouti lethal yellow (KK.Cg-Ay/J) mice, an excellent model for progressive obesity [46–48]. The impact of obesity onset and progression on expression of ovarian genes encoding insulin signaling, PI3K pathway members, and enzymes involved in ovarian xenobiotic biotransformation were investigated. Additionally, we challenged both lean and obese mice with the ovotoxicant, phosphoramide mustard (PM; the ovotoxic metabolite of cyclophosphamide [CPA]), and evaluated the response of EPHX1 to PM exposure in ovarian and lung tissue.

Materials and methods

Reagents

Phosphoramide mustard was obtained from the National Institutes of Health National Cancer Institute (Bethesda, MA). D-Glucose, 2-beta-mercaptoethanol, 30% acrylamide/0.8% bis-acrylamide, ammonium persulfate, glycerol, N′,N′,N′,N′-Tetramethyl-ethylenediamine, Tris base, Tris HCl, sodium chloride, Tween-20, bovine serum albumin (BSA), ascorbic acid (vitamin C), phosphatase inhibitor, protease inhibitor, and transferrin were purchased from Sigma-Aldrich Inc. (St. Louis, MO). Custom designed primers were obtained from the DNA facility of the Office of Biotechnology at Iowa State University. Hanks balanced salt solution (without $CaCl_2$, $MgCl_2$, or $MgSO_4$) and superscript III one-step real-time polymerase chain reaction (RT-PCR) System were purchased from Invitrogen Co. (Carlsbad, CA). RNA*later* was obtained from Ambion Inc. (Austin, TX). RNeasy Mini kit, QIAshredder kit, RNeasy MinElute kit, and QuantiTect SYBR Green PCR kit were purchased from Qiagen Inc. (Valencia, CA). Ponceau S was purchased from Fisher Scientific (Waltham, MA). Restore PLUS Western Blot Stripping Buffer was purchased from Thermo Scientific (Rockford, IL). SignalFire ECL Reagent, goat anti-rabbit secondary antibody, anti-pAKT^{Thr308}, and anti-pIRS1^{Ser302} antibodies were from Cell Signaling Technology (Danvers, MA). Anti-FOXO3 and anti-GSTP1 antibodies were purchased from Millipore (Temecula, CA). Donkey anti-goat secondary antibody was purchased from Pierce Biotechnology (Rockford, IL). Anti-CYP2E1 antibody was purchased from Abcam (Cambridge, MA). Anti-mEH (EPHX1) antibody was purchased from Detroit R&D, Inc. (Detroit, M).

Animal procedures and tissue collection

All experimental animal protocols used in this study were approved by the Iowa State University Animal Care Committee. Four-week-old female normal wild-type nonagouti (a/a; designated lean; n = 20) and agouti lethal yellow (KK.Cg-Ay/J; designated obese; n = 20) mice were purchased from the Jackson Laboratory (Bar Harbor,

Table 1. Primer sequences used for quantitative RT-PCR.

Gene name	Forward primer sequence (5′-3′)	Reverse primer sequence (5′-3′)
Irs2	GAA GCG GCT AAG TCT CAT GG	GAC GGT GGT GGT AGA GGA AA
Irs3	TCG GCT CAC CGT TTC CTT G	TCG CTC TCG TAG CAC TCC A
Akt2	TGG ACC ACA GTC ATC GAG AG	CTT GTA ATC CAT GGC GTC CT
Foxo1	GAG TGG ATG GTG AAG AGC GT	TGC TGT GAA GGG ACA GAT TG
Foxo3a	CTG GGG GAA CCT GTC CTA TG	TCA TTC TGA ACG CGC ATG AAG

Maine) as previously described [45]. The mice were housed at the animal facility at Iowa State University under identical conditions of room temperature (21°C–22°C), lighting (12 h light:12 h darkness cycle), and ad libitum access to feed and water until 6, 12, 18, or 24 weeks of age. Phenotypically, the lethal yellow mice had elevated body weight (42.2, 43.2, 48 g at 12, 18, and 24 weeks, respectively [45]), and fasting glucose levels from 12 weeks onwards [45]. Estrous cyclicity was also impacted by shorter time spent in estrus and longer time in diestrous [45]. In addition, primordial and small primary follicle numbers were decreased, while secondary and antral follicle numbers were increased in number with progressive obesity [45]. At the end of each experimental time point, mice were euthanized by CO_2 asphyxiation in the proestrus stage of the estrous cycle as determined by vaginal cytology. Ovaries were collected, cleaned of excess fat, and stored in RNA*later* at –80°C for RNA and protein analyses.

In vivo phosphoramide mustard exposure and tissue collection

A separate group of normal wild-type nonagouti (a/a; designated lean; n = 10) and agouti lethal yellow (KK.Cg-Ay/J; designated obese; n = 10) mice aged 15 weeks were intraperitoneally (ip) dosed once with sesame oil or PM (95%; 25 mg/kg) (n = 5 per group). This dose was chosen based on the literature to cause primordial follicle loss, but not to completely eliminate the follicular pool [49]. Mice were euthanized 3 days after the end of dosing in their proestrus phase of the estrous cycle as determined by vaginal cytology. Ovary and lung tissue from each mouse was preserved in RNA*later* at –80°C for RNA and protein isolation.

RNA isolation, first-strand cDNA synthesis, and quantitative real-time polymerase chain reaction

Total RNA was isolated from both lean and obese mice using Qiagen RNeasy Mini Kit (at 6, 12, 18, and 24 weeks, n = 3–4 per group per time point) as per the manufacturer's protocol [45]. Briefly, ovaries were lysed and homogenized using a hand-held homogenizer followed by applying the homogenate to a QIAshredder column with subsequent centrifugation at 16100 RCF for 2 min at room temperature. The resulting supernatant was applied to an RNeasy Mini column, allowing RNA to bind to the filter cartridge. Following washing, RNA was eluted from the filter and concentrated using an RNeasy MinElute Kit according to the manufacturer's protocol. The total RNA was eluted using 14 μL of RNase-free water and concentration determined using an ND-1000 Spectrophotometer (λ = 260/280 nm; NanoDrop technologies, Inc., Wilmington, DE). For cDNA synthesis, RNA (0.5 μg) was reverse-transcribed using Invitrogen Superscript III Reverse Transcriptase according to the manufacturer's protocol. cDNA (2 μL; 1:25 dilution) was amplified on an Eppendorf Mastercycler using a Quantitect SYBR Green PCR kit and primers specific for mouse *Gapdh*, *Insr*, *Irs1, Kitlg, cKit, Akt1, Gstm1, Gstp1, Ephx1, and Cyp2e1* (see sequences in [36]), *Irs2, Irs3, Akt2, Foxo1, and Foxo3a* (for sequences see Table 1). The PCR cycling program consisted of a 15-min hold at 95°C and 40 cycles of denaturing for 15 at 95°C, annealing for 15 s at 58°C, and extension at 72°C for 20s. Product melt conditions were determined using a temperature gradient from 72°C to 99°C with a 1°C increase at each step. A single product was confirmed per reaction. Three replicates of each sample were included. The relative mRNA expression for each gene was normalized using the housekeeping gene *Gapdh* and relative fold-change calculated using the $2^{-\Delta\Delta CT}$ method. The results are presented as mean fold-change ± standard error relative to the lean-matched control group.

Protein isolation and western blot analysis

At each time point (6, 12, 18, or 24 weeks of age, n = 3–4 per group per time point), total ovarian protein was isolated and western blotting was performed as previously described [45]. Ovaries were homogenized in 300 μL of ice-cold tissue lysis buffer and protein concentration quantified using a standard bicinchoninic acid protocol on a 96-well assay plate. Equal total protein (20 μg) was separated on a 10%–12% SDS-PAGE and subsequently transferred to nitrocellulose membranes. Ponceau S staining was performed to visualize and confirm equal amount of protein loading and transfer. Following blocking for 2 h at room temperature, membranes were probed with specific primary antibodies [Rabbit Anti-GSTP1 (1:200), Goat anti-EPHX1 (1:500), Rabbit anti-pIRS1^{Ser302} (1:200), Rabbit anti-pAKT^{Thr308} (1:250), Rabbit anti-FOXO3 (1:250), Rabbit anti-CYP2E1 (1:200)] in 5% BSA in TTBS for 24–48 h at 4°C. HRP-conjugated secondary antibodies (1:10000 – 1:20000) were added for 1 h at room temperature, and membrane-bound HRP was washed three consecutive times for 5 min each time in TTBS. Autoradiograms were visualized on X-ray film following 10-min incubation of membranes with 1X SignalFire ECL reagent. Densitometry of the appropriate sized bands was measured using Carestream Molecular Imaging software version 5.0 (Carestream Health Inc., Rochester, NY) which eliminates background noise. Densitometric values of appropriate target proteins were normalized to Ponceau S staining prior to statistical analysis.

Statistical analysis

Statistical analyses were performed using the unpaired *t*-test function of GraphPad Prism 5.5 software with a statistical significance level set at $P < 0.05$. A trend toward a biologically meaningful difference between treatments was considered if the *P*-value was less than 0.1.

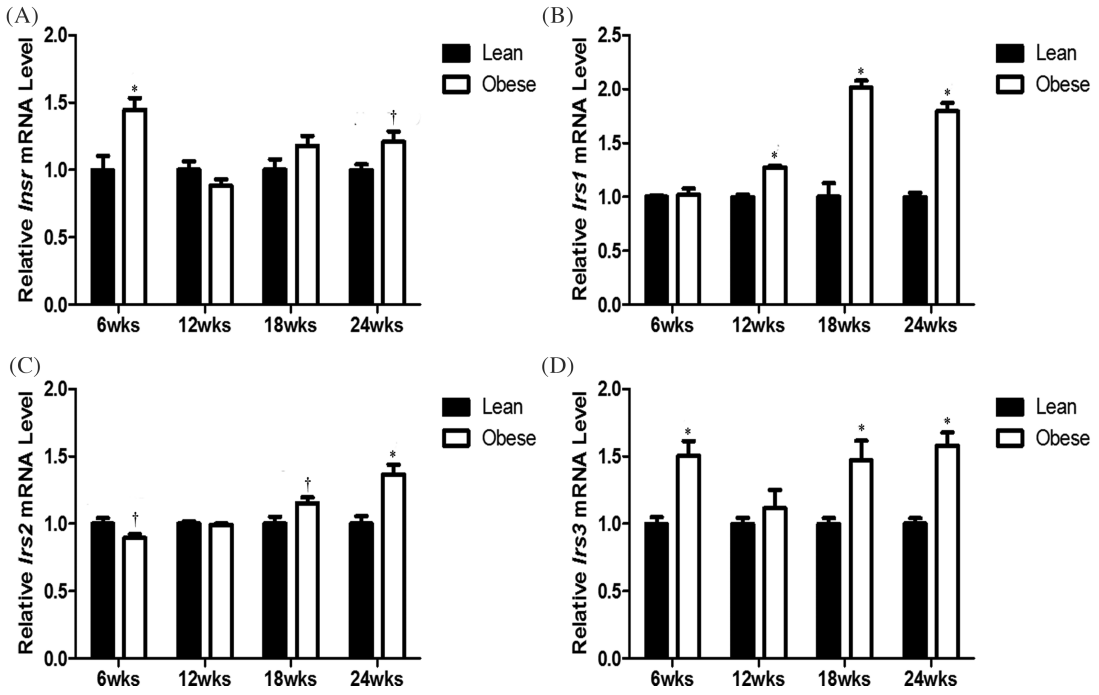

Figure 1. Obesity increases ovarian mRNA expression of insulin signaling members. Total ovarian RNA was isolated from lean or obese mice at 6, 12, 18, or 24 weeks (n = 4, per group per time point), reverse transcribed, and qRT-PCR performed to quantify mRNA levels of (A) *Insr*, (B) *Irs1*, (C) *Irs2*, and (D) *Irs3*. Target gene mRNA expression values were normalized to *Gapdh* as a housekeeping gene. Results are presented as relative fold-change means ± SEM. Asterisk indicates significant difference from age-matched lean females at $P < 0.05$; dagger indicates $P < 0.1$.

Results

Obesity increases ovarian mRNA expression of insulin signaling members

Since obese mice displayed reduced glucose clearance rate in addition to having higher fasting blood glucose levels [45], we sought to determine the impact of progressive obesity on ovarian mRNA expression of insulin signaling members. At 6 weeks of age, ovaries from the obese mice had increased *Insr* (Figure 1A, $P < 0.05$) and *Irs3* (Figure 1D, $P < 0.01$) but showed no difference in either *Irs1* or *Irs2* mRNA levels relative to ovaries from the lean mice. At 12 weeks, only *Irs1* mRNA was increased (Figure 1B, $P < 0.001$) with obesity but other members were not impacted by obesity. Similarly, ovaries from obese mice displayed increased *Irs1* (Figure 1B, $P < 0.001$) and *Irs3* (Figure 1D, $P < 0.05$) without significant effect on *Insr* (Figure 1A) and *Irs2* (Figure 1C) mRNA levels at 18 weeks of age. In the 24-week-old group, obesity increased ovarian expression of *Insr* (Figure 1A, $P = 0.05$), *Irs1* (Figure 1B, $P < 0.0001$), *Irs2* (Figure 1C, $P < 0.01$), and *Irs3* (Figure 1D, $P < 0.01$).

Progressive obesity increases ovarian phosphorylated insulin receptor substrate 1 protein

Following the impact of obesity on ovarian mRNA levels of insulin signaling members, we investigated protein levels of pIRS1^{Ser302} (Figure 2). Although there was no difference in phosphorylation of IRS1 protein at the serine 302 site at 6 weeks, relative to lean-matched controls, ovaries from obese mice showed a tendency for increased pIRS1^{Ser302} protein levels at 12 weeks ($P = 0.07$), and increased protein at 18 ($P < 0.05$) and 24 ($P < 0.01$) weeks (Figure 2).

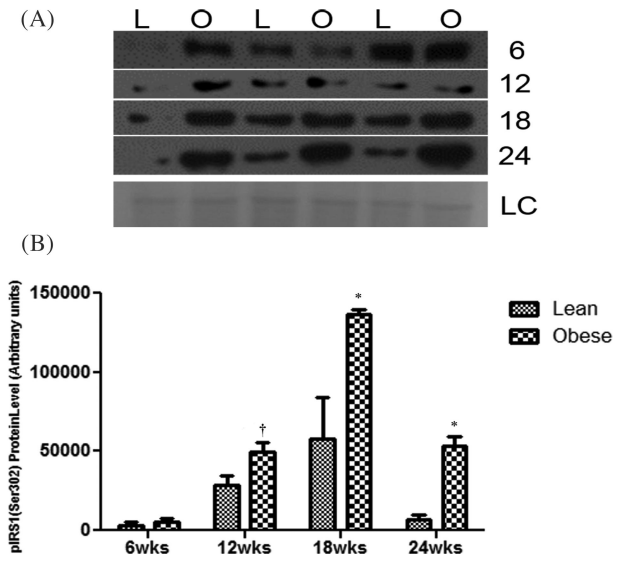

Figure 2. Progressive obesity increases ovarian phosphorylated insulin receptor substrate 1 protein. Total ovarian protein was isolated from lean (L) and obese (O) mice at 6, 12, 18, or 12 weeks (n = 3–4 per group per time point). Protein expression of pIRS1^{Ser302} was determined by western blotting, followed by densitometric quantification of the appropriate protein band using Carestream Molecular Imaging software. Bars represent means ± SEM in arbitrary units. Asterisk indicates significant difference from age-matched lean females at $P < 0.05$; dagger indicates $P < 0.1$.

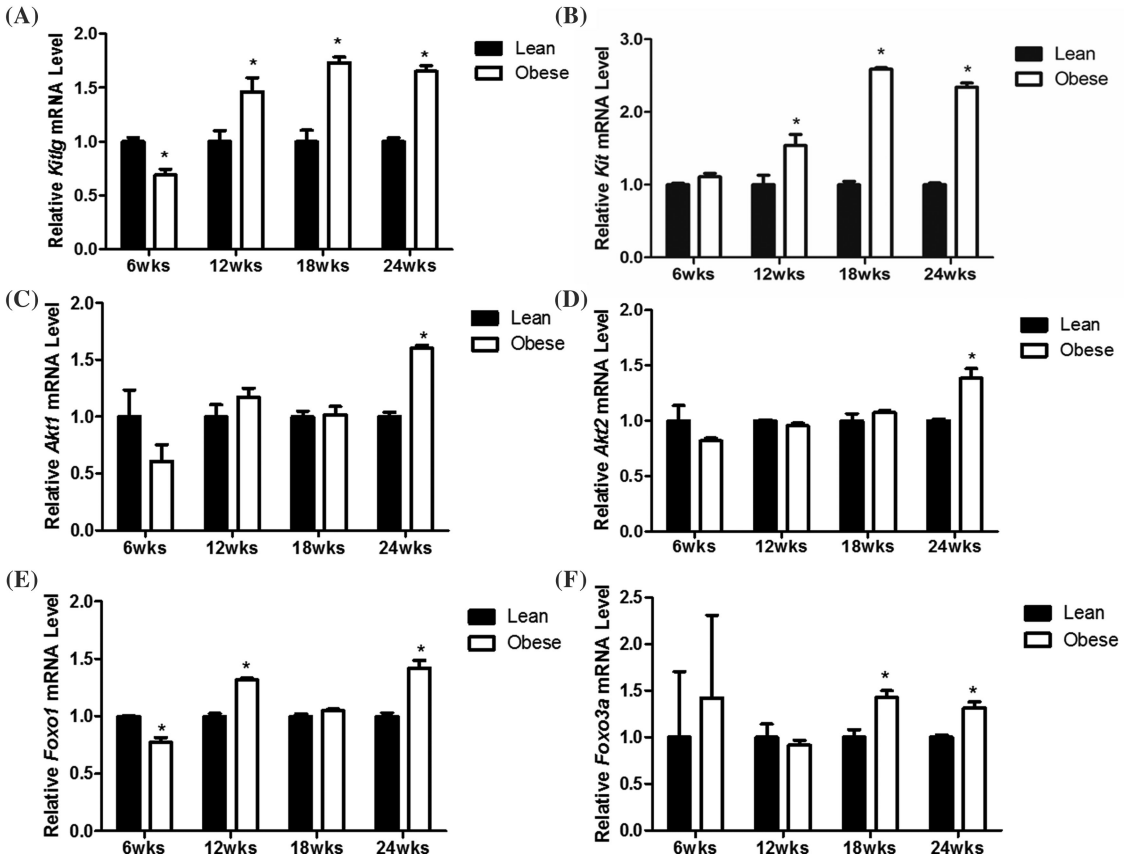

Figure 3. Ovarian Kitlg/Kit-PI3K pathway members are elevated during obesity. Total ovarian RNA was isolated from lean or obese mice at 6, 12, 18, or 24 weeks (n = 4, per group per time point), reverse transcribed, and qRT-PCR performed to quantify the mRNA levels of (A) *Kitlg,* (B) *Kit,* (C) *Akt1,* (D) *Akt2* (E) *Foxo1,* and (G) *Foxo3a.* Target gene mRNA expression values were normalized to *Gapdh* as a housekeeping gene. Results are presented as relative fold-change means ± SEM. Asterisk indicates significant difference from age-matched lean females at $P < 0.05$.

Ovarian Kitlg/cKit-PI3K pathway members are elevated during obesity

At 6 weeks, ovaries from the obese group had lower ($P < 0.01$) *Kitlg* (Figure 3A) and *Foxo1* (Figure 3E) but not *Kit*, *Akt1, Akt2,* or *Foxo3a* mRNA levels than ovaries from lean females (Figure 3). At 12 weeks, there was a marked increase in ovarian *Kitlg* (Figure 1A, $P < 0.05$), *Kit* (Figure 1B, $P < 0.05$), and *Foxo1* (Figure 1E, $P < 0.0001$) in obese compared to lean females, but there was no impact of obesity on *Akt1* (Figure 3C), *Akt2* (Figure 3D), or *Foxo3a* (Figure 3F) mRNA expression. Likewise, at 18 weeks, obesity did not affect ovarian *Akt1* (Figure 3C), *Akt2* (Figure 3D), and *Foxo1* (Figure 3E) mRNA levels, but increased *Kitlg* (Figure 3A, $P < 0.001$), *Kit* (Figure 3B, $P < 0.0001$), and *Foxo3a* (Figure 3E, $P < 0.01$) mRNA levels. There was increased ($P < 0.01$) *Kitlg, Kit, Akt1, Akt2, Foxo1,* and *Foxo3a* mRNA levels in ovaries from obese compared to lean mice at 24 weeks (Figure 3A–F).

Ovarian phosphorylated AKT is increased by obesity without impacting FOXO3 protein levels

There were no differences in ovarian $pAKT^{Thr308}$ protein levels between lean and obese females at 6 and 12 weeks, but obesity increased ($P < 0.01$) $pAKT^{Thr308}$ protein expression at 18 and 24 weeks (Figure 4A). Total ovarian FOXO3A protein levels did not differ between lean and obese groups at any time points (Figure 4B).

Progressive obesity alters mRNA expression of ovarian xenobiotic metabolism genes

Despite lack of a genotype effect on *Gstm1, Gstp1,* and *Ephx1* mRNA levels at 6 weeks [50], obesity increased ($P < 0.001$) ovarian *Gstm1* (Figure 5A) and *Ephx1* (Figure 5C) mRNA expression at 12, 18, and 24 weeks. On the contrary, ovarian *Cyp2e1* mRNA expression was lower ($P < 0.001$) in the obese group at all of the time points investigated (Figure 5D). *Gstp1* mRNA levels were decreased ($P < 0.05$) by obesity at 12 weeks; however, at 24 weeks there was a tendency ($P = 0.06$) for increased ovarian *Gstp1* in obese versus lean females (Figure 5B). At 18 weeks, there was no difference between lean and obese females in ovarian *Gstp1* mRNA levels (Figure 5B).

Abundance of ovarian xenobiotic metabolism proteins is impacted by increased body mass

At 6 weeks, there was no difference in ovarian EPHX1, CYPE1, and GSTP1 protein levels between the two groups of mice (Figure 6). Relative to their matched lean controls, obese females displayed a higher ($P < 0.05$) expression of ovarian GSTP1 at 18 and 24 weeks (Figure 6A and C). In a similar manner to the mRNA results, ovaries from obese mice had increased ovarian EPHX1 protein levels relative to their lean counterparts at 12 ($P < 0.05$), 18 ($P < 0.01$), and 24 ($P < 0.0001$) weeks (Figure 6B and D). Likewise, CYP2E1 protein expression was reduced in ovaries from obese females compared to

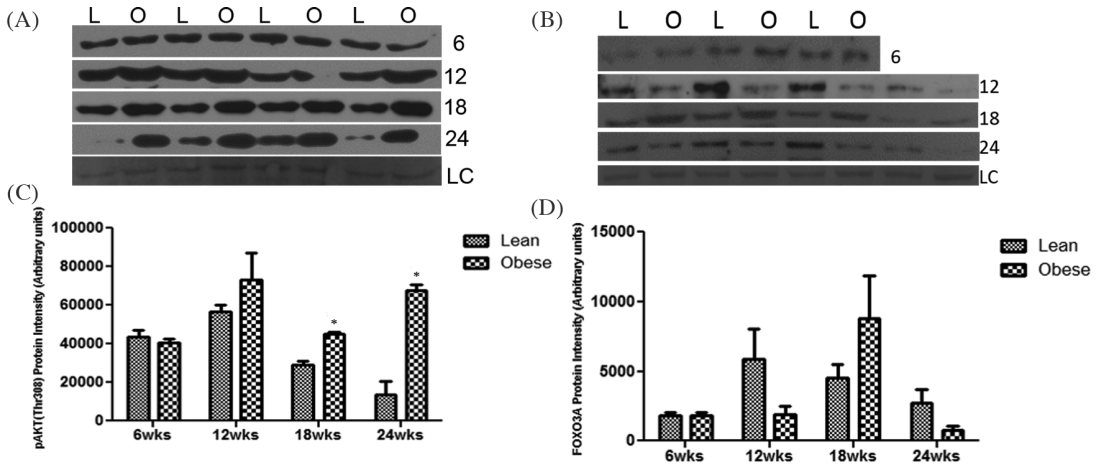

Figure 4. Ovarian phosphorylated AKT is increased by obesity without impacting FOXO3 protein levels. Total ovarian protein was isolated from lean (L) and obese (O) mice at 6, 12, 18, or 12 weeks (n = 3–4 per group per time point). Protein expression was determined by western blotting, followed by densitometric quantification of the appropriate protein bands using Carestream Molecular Imaging software. (A) pAKT^{Thr308} and (B) FOXO3 protein levels. Bars represent means ± SEM in arbitrary units. Asterisk indicates significant difference from age-matched lean females at $P < 0.05$.

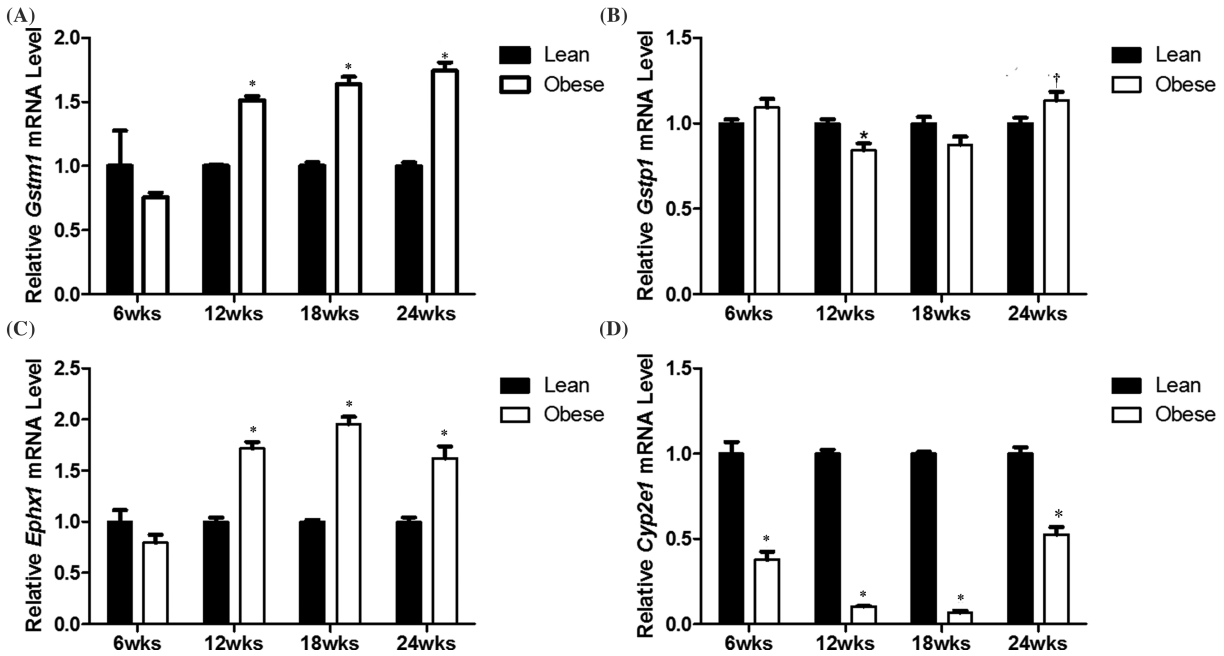

Figure 5. Progressive obesity alters mRNA expression of ovarian xenobiotic metabolism genes. Total ovarian RNA was isolated from lean or obese mice at 6, 12, 18, or 24 weeks (n = 4, per group per time point), reverse transcribed, and quantitative RT-PCR performed to quantify the mRNA levels of (A) *Gstm1*, (B) *Gstp1*, (C) *Ephx1*, and (D) *Cyp2e1*. Target gene mRNA expression values were normalized to *Gapdh* as a housekeeping gene. Results are presented as relative fold-change means ± SEM. Asterisk indicates significant difference from age-matched lean females at $P < 0.05$; dagger indicates $P < 0.1$.

their lean littermates at 12 ($P < 0.01$), 18 ($P < 0.05$), and 24 ($P < 0.01$) weeks (Figure 6E and F).

Obesity alters ovarian EPHX1 in response to phosphoramide mustard exposure

Lean mice exposed to PM had increased ($P < 0.05$) ovarian EPHX1 protein abundance (Figure 7A). Concurrent with our previous observations [50], obese females had basally higher ($P < 0.05$) levels of ovarian EPHX1 relative to ovaries from lean mice. In contrast to ovaries from lean mice, the EPHX1 response to PM exposure was completely abrogated in obese mice (Figure 7A).

In lung tissue from lean and obese mice dosed with PM, there was increased EPHX1 protein abundance (Figure 7B); however, the response in the obese mice tended toward significance ($P < 0.1$) while the response observed in the lean mice was greater ($P < 0.05$; Figure 7B).

Discussion

Obese mothers have increased risk for miscarriage [51], poor oocyte quality [52], and birth defects in their offspring [51]. In a recent study, we discovered that ovaries from obese females may have

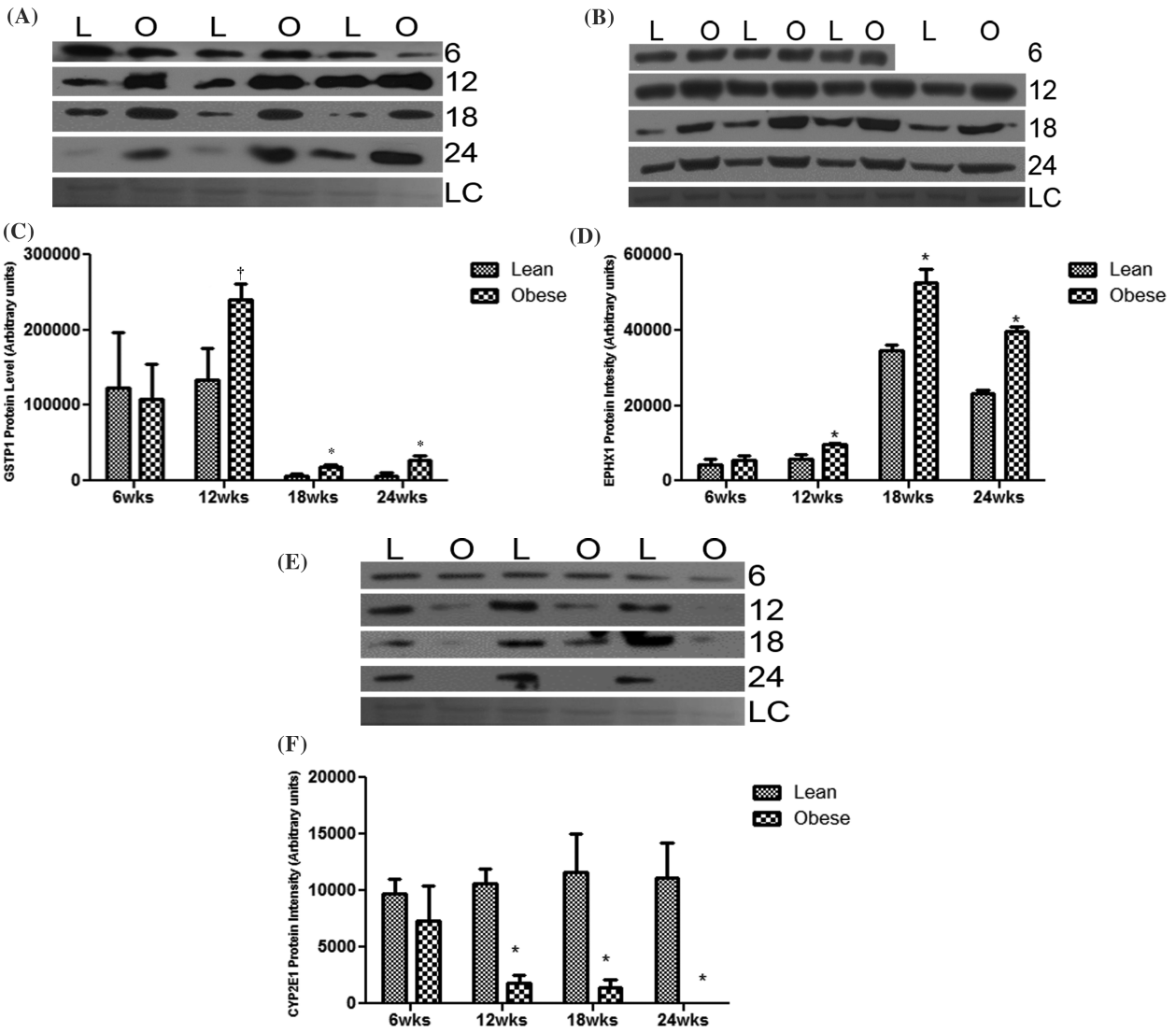

Figure 6. Abundance of ovarian xenobiotic metabolism proteins is impacted by increased body mass. Total ovarian protein was isolated from lean (L) and obese (O) mice at 6, 12, 18, or 12 weeks (n = 3–4 per group per time point). Protein expression was determined by western blotting, followed by densitometric quantification of the appropriate protein band using Carestream Molecular Imaging software. (A, C) GSTP1, (B, D) EPHX1, and (E, F) CYP2E1 protein levels. Bars represent means ± SEM in arbitrary units. Asterisk indicates significant difference from age-matched lean females at $P < 0.05$; dagger indicates $P < 0.1$.

increased susceptibility to environmental exposures due to increased levels of EPHX1 and altered GST levels [50]. Additionally, obese females had greater ovarian damage induced by the ovotoxicant 7,12-dimethylbenz[a]anthracene [50]. Although the mechanism(s) remain unclear, we propose that ovarian biotransformation capacity may be altered during obesity, leading to increased susceptibility to ovotoxicant effects. Additionally, in a study of progressive obesity, we demonstrated a reduction in preantral follicles in obese females [45]. Since roles for PI3K signaling in oocyte viability [53], primordial follicle activation [54–59], and ovarian chemical metabolism [24, 25, 43] have been established, we also hypothesized that impacts on ovarian biotransformation capacity during obesity may be mediated through altered insulin-regulated PI3K signaling. Since our previous study investigated a single time point [50], we chose a model of progressive obesity in which to determine impacts of obesity onset and establishment on the endpoints of interest.

Many rodent models of obesity have mutations in the satiety hormone leptin (*ob/ob*) [60] or its receptor (*db/db*) [61]. While these mutations result in rapid onset of obesity, they are rare in the human population [48, 62]. The lethal yellow mouse has a deletion mutation in the normal wild-type nonagouti (a/a) background which results in ectopic expression of agouti [46, 48, 63, 64]. Hypothalamic agouti overexpression inhibits the melanocyte stimulating hormone (MSH) receptor [65] leading to hyperphagia due to hindering of the inhibitory effects of feeding imparted by alpha-melanocyte-stimulating hormone (α-MSH) and cocaine- and amphetamine-regulated transcript [65, 66]. Subsequently, hyperphagia coupled with reduced energy expenditure results in the development of progressive obesity [46, 65]. Starting at 12 weeks of age, these mice are hyperinsulinemic [47] and hyperleptinemic [67], and display insulin [46] and leptin [68] resistance. Additionally, premature reproductive failure is a common phenotype of the lethal yellow mouse [67, 69, 70]. Elevated insulin levels have been reported in both serum and follicular fluids

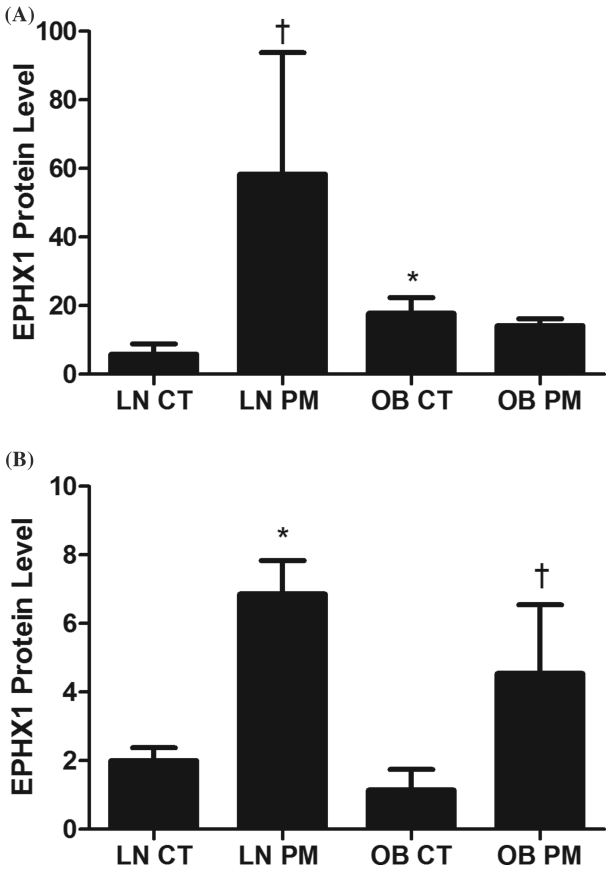

Figure 7. EPHX1 is increased in lean but not obese ovaries in response to PM exposure. Total ovarian protein was isolated from lean (L) and obese (O) mice at dosed with PM at 15 weeks of age (n = 3–4 per group per time point). Protein expression was determined by western blotting, followed by densitometric quantification of the appropriate protein band using Carestream Molecular Imaging software. (A) Ovarian and (B) lung EPHX1 protein abundance. Bars represent means ± SEM in arbitrary units. Asterisk indicates significant difference from age-matched lean females at $P < 0.05$; dagger indicates $P < 0.1$.

of obese females [71, 72]. However, studies investigating whether the ovary retains insulin sensitivity during hyperinsulinemia are contradictory [36, 38, 39, 73]. We chose to perform evaluation of effects of obesity on ovarian PI3K and chemical metabolism signaling at 6, 12, 18, and 24 weeks of age, since these ages have been characterized in this model [47] and we have established the composition of the follicular pool at these same endpoints [45].

Progressive obesity was associated with increased *Irs1*, *Irs2,* and *Irs3* mRNA as well as pIRS1^{Ser302} protein levels, perhaps indicating that ovarian insulin signaling pathway retains activity in ovaries from obese mice, supporting our previous data with both high fat diet-fed mice [36] and the lethal yellow mouse [45]. The IRS1 contains several tyrosine/serine phosphorylation sites that serve as docking sites for numerous downstream mediators of insulin growth-promoting and metabolic functions [74–77]. Although most serine phosphorylations of IRS lead to insulin signaling attenuation [76], phosphorylation of IRS1 at serine 302 in rodents, which corresponds to serine 307 of the human IRS1 [78, 79], is associated with insulin stimulation and it is believed to have a positive action in subsequent IRS1 tyrosine phosphorylations [77–79]. In several studies, inhibition of pIRS1^{Ser302} by glucose starvation or deprivation of short-term amino acid correlates with decreased IRS1 tyrosine phosphorylation and subsequent reduced insulin activity [76, 77, 80]. Also increased pIRS1^{Ser302} has been observed during peripheral insulin resistance in the skeletal muscle of both rodents [81] and humans [82, 83]. Whether the observed increase in ovarian pIRS1^{Ser302} protein levels during progressive obesity in this study represents positive or negative feedback to insulin stimulation is hard to discern, but provides further evidence that ovarian insulin signaling is sustained during obesity.

In cultured human ovarian cortex, insulin alone or in combination with IGF-I and IGF-II increased the percentage of primordial follicles transitioning to the primary stage [84]. In canines [85] and fetal hamster cultured ovaries [86], elevated insulin concentrations activated preantral follicular growth and viability, while insulin also promoted the transition from primordial to primary follicle stage in rat ovaries [87] and bovine cortical pieces [88]. Moreover, insulin had an additive effect with Kit Ligand (KITLG) on increasing follicle activation in cultured neonatal rat ovaries [87, 89]. These studies suggest a functional role for insulin signaling in ovarian folliculogenesis regulation. Insulin acting through its receptor and the receptor substrate proteins can activate the PI3K-AKT-dependent signaling pathway [90]. AKT activation involves two phosphorylations: one at threonine 308 (Thr308) normally by phosphoinositide-dependent kinase (PDPK1) and the other at serine 473 (Ser473) by mammalian target of rapamycin complex 2 (mTORC2) [91–93]. In mouse liver [94] or skeletal muscle [95] lacking IRS1 or IRS2, AKT Thr308 phosphorylation (pAKT^{Thr308}) is undetectable; however, AKT phosphorylation at Ser473 (pAKT^{Ser473}) is retained [96], thus pAKT^{Ser473} may not be the most sensitive indicator of IRS-mediated PI3K-AKT signaling [91, 97]. We demonstrate increased pAKT^{Thr308} with obesity progression indicating increased PI3K-AKT activation in obese females. FOXO3 is a downstream AKT target that is negatively regulated upon AKT activation [28, 92, 98, 99]. We noted a trend for a 60% and 70% reduction in this protein in ovaries from obese mice at 12 and 24 weeks, respectively, suggestive of increased activation of insulin-PI3K/AKT signaling pathway during progressive obesity. Hyperactivation of the PI3K-AKT-FOXO3 signaling pathway has been shown to increase the rate of primordial follicles activation and recruitment into the growing pool with eventual death of most of those follicles, leading to accelerated ovarian senescence [30, 57, 59, 100, 101]. In support of this posit, we previously demonstrated reduced follicle numbers due to obesity from 12 weeks onward in the lethal yellow mouse model [45].

In addition to insulin, PI3K-AKT-FOXO3a can be activated by KITLG through its protein-tyrosine kinase receptor, KIT [98, 102, 103]. *Kit* is expressed in the oocyte [104–106], whereas *Kitlg* originates from the GC and TC [88, 107, 108]. In the ovary, KITLG binding to KIT induces phosphorylation of the regulatory subunit of PI3K and subsequent activation of AKT1 [98, 102, 103]. We previously found that that HFD-induced obesity increased *Kitlg* concomitant with increased *Akt1* and decreased *Foxo3a* mRNA expression in murine ovaries [36]. In this study, we also observed increased ovarian *Kit* and *Kitlg* mRNA concomitant with increased pAKT^{Thr308} protein in obese mice relative to their lean littermates. The ovarian KITLG-KIT pathway plays a pivotal role in regulation of ovarian folliculogenesis [107, 109–114] and steroidogenesis [115]. In human ovarian follicles, blocking the KIT receptor using an anti-KIT antibody, ACK2, induced ovarian follicular atresia [116]. KITLG supplementation promoted the transition of primordial to the primary follicle stage in bovine ovarian cortical pieces [114], and stimulated follicle activation in rodents [110, 112]. Taken together,

our data support that activation of insulin-KITLG-KIT-AKT1 signaling pathway is induced by obesity, and this could be a potential mechanism underlying obesity-induced overactivation of primordial follicles into the growing follicular pool previously noted in both this mouse model [50] and rats [40].

In primary cultured rat hepatocytes, insulin administration decreased *Cyp2e1* mRNA expression in a dose-dependent manner, and this was reversible by either addition of glucagon or PI3K inhibitors (Wortmannin or LY294002) [117, 118]. Increased *Cyp2e1* mRNA and/or CYP2E1 protein abundance have been reported during diabetes [119–121], glucagon treatment [117], and starvation [120, 122], physiological states that are normally associated with decreased insulin activity. Interestingly, EPHX1 expression pattern is opposite to CYP2E1 during these physiological states. Insulin treatment or refeeding increases *Ephx1* mRNA, EPHX1 protein expression, and enzyme activity [122–124]; however, diabetes [122, 124], glucagon [123], or starvation [122, 124] or PI3K inhibition [123] decreases *Ephx1* expression. Similar to the liver, opposing expression patterns of ovarian EPHX1 and CYP2E1 expression have been previously reported [21, 36]. In this study, similar to the mRNA results, there was an increase in ovarian EPHX1 with a concomitant decrease in CYP2E1 protein levels in ovaries from obese females compared to their age-matched lean counterparts.

In a similar manner to EPHX1 and CYP2E1, the expression and activities of GST enzymes can be mediated through PI3K/AKT signaling [24, 125, 126]. In male rats, the addition of insulin reversed decreased hepatic GST activity that had been induced by diabetes [124]. Also, refeeding (associated with insulin stimulation) restored starvation-induced reduced liver GST enzyme activities [124]. We recently observed increased ovarian levels of *Gstm1* mRNA, GSTM1 and GSTP1 proteins due to an obese phenotype [50]. In the data reported herein, we observed an increase in ovarian *Gstm1* mRNA and GSTP1 protein expression with progressive obesity. GSTs are critical for detoxification of a number of xenobiotic compounds [24, 127, 128]. In addition, ovarian GSTP1 [15, 24] and GSTM1 [25] negatively regulate proapoptotic proteins; thus, their increased level in obesity may reflect a reduction in apoptosis during obesity. Both these functions are in agreement with GSTP1 and GSTM1 being implicated in susceptibility toward and poor prognosis from various forms of gynaecological tumours [125, 129, 130] and development of anticancer drug resistance [131–135]. Therefore, increased abundance of ovarian GSTM1 and GSTP1 during obesity could be part of the underlying mechanisms behind obesity-induced reproductive disorders in obese females.

In order to increase translatability of our findings to this point, we evaluated the impact of obesity on ovarian chemical biotransformation and challenged the lean and obese mice with PM, an ovotoxic metabolite of CPA. The single dose was based on an early study investigating ovotoxicity of PM [49] with our aim being to induce mild levels of follicle loss. Also, we had determined in another study that this PM dosage reduced ovarian weight in obese but not lean mice [136]. Additionally, both lean and obese mice had reduced primordial follicle number and DNA damage in response to PM. Interestingly, DNA repair was blunted in the obese female ovary in response to PM-induced DNA damage [136]. We have previously demonstrated that EPHX1 protein detoxifies PM [137]; when EPHX1 was inhibited in cultured rat ovaries, greater PM-induced follicle loss was observed [137], and thus the ovary responded to a single dose of PM exposure in terms of increased EPHX1. Thus, in this study, we evaluated whether obesity affected the ovarian EPHX1 response to PM exposure. Interestingly, comparison of the level of ovarian EPHX1 between obese and lean mice identified increased basal EPHX1 protein abundance in the obese mice. We had previously reported this finding in a separate experiment [50], and these data further underscore that ovaries from obese females have altered potential for chemical biotransformation. Additionally, we discovered that, despite a higher basal EPHX1 level in ovaries from obese females, the response to PM exposure was essentially absent; thus, ovaries from obese females have the potential for reduced detoxification of the ovotoxicant PM during chemotherapy regimens that include CPA, thereby increasing ovarian damage that ensues. In order to further extend our findings, we investigated whether lung tissue was responsive to PM exposure. We have determined that PM can spontaneously transform into a volatile ovotoxicant [138], and a study determined that a portion of administered CPA was expired from the lungs of treated animals as chloroethylaziridine [139]. We observed increased abundance of EPHX1 in the lungs of both lean and obese females and did not observe any notable difference due to obesity. Thus, these data could indicate that a volatile compound results from PM exposure in vivo and is an area for further exploration. Furthermore, the differences in EPHX1 response to PM between the lung and ovary underscore tissue-specific responses to chemical exposure.

Taken together, our data demonstrate that progressive obesity increased mRNA and/or protein of ovarian signaling pathways that regulate folliculogenesis and ovotoxicant metabolism. These findings are of concern since dysregulated activation of follicles into the growing pool will eventually result in their depletion, accelerating entry into ovarian senescence. In addition, altered ovarian capacity to biotransform chemicals could pose a threat to both folliculogenesis and stability of the germ line. It is noteworthy that the "lean" mice also experience increased body weight with aging; thus, the obesity-induced effects on ovarian physiology may be changes that occur with aging, but are happening at a more rapid rate. It would be of interest to determine if exercise of diet-induced weight loss could mitigate the obesity-induced ovarian effects and this is an area of interest for this group. We further demonstrated that the obese ovary has a compromised response in terms of EPHX1 induction in response to PM exposure which could translate into a worsened outcome for obese patients during anticancer therapies involving CPA.

Declaration of interest

There are no conflicts of interest to declare.

References

1. Brewer CJ, Balen AH. The adverse effects of obesity on conception and implantation. *Reproduction* 2010; **140**:347–364.
2. Kulie T, Slattengren A, Redmer J, Counts H, Eglash A, Schrager S. Obesity and Women's Health: an evidence-based review. *J Am Board Fam Med* 2011; **24**:75–85.
3. Zaadstra BM, Seidell JC, Van Noord PA, te Velde ER, Habbema JD, Vrieswijk B, Karbaat J. Fat and female fecundity: prospective study of effect of body fat distribution on conception rates. *BMJ* 1993; **306**:484–487.
4. Crosignani PG, Ragni G, Parazzini F, Wyssling H, Lombroso G, Perotti L. Anthropometric indicators and response to gonadotrophin for ovulation induction. *Hum Reprod* 1994; **9**:420–423.
5. Rachoń D, Teede H. Ovarian function and obesity—Interrelationship, impact on women's reproductive lifespan and treatment options. *Mol Cell Endocrinol* 2010; **316**:172–179.

6. Rich-Edwards JW, Goldman MB, Willett WC, Hunter DJ, Stampfer MJ, Colditz GA, Manson JE. Adolescent body mass index and infertility caused by ovulatory disorder. *Am J Obstet Gynecol* 1994; **171**: 171–177.
7. Edlow AG, Vora NL, Hui L, Wick HC, Cowan JM, Bianchi DW. Maternal obesity affects fetal neurodevelopmental and metabolic gene expression: a pilot study. *PLoS One* 2014; **9**:e88661.
8. Correa A, Marcinkevage J. Prepregnancy obesity and the risk of birth defects: an update. *Nutr Rev* 2013; **71**(Suppl 1):S68–S77.
9. Block SR, Watkins SM, Salemi JL, Rutkowski R, Tanner JP, Correia JA, Kirby RS. Maternal pre-pregnancy body mass index and risk of selected birth defects: evidence of a dose-response relationship. *Paediatr Perinat Epidemiol* 2013; **27**:521–531.
10. Ogden CL, Carroll MD, Fryar CD, Flegal KM. Prevalence of obesity among adults and youth: United States, 2011–2014. NCHS Data Brief, no 219. Hyattsville, MD: National Center for Health Statistics; 2015.
11. Hirshfield AN. Development of follicles in the mammalian ovary. *Int Rev Cytol* 1991; **124**:43–101.
12. Bhattacharya P, Keating AF. Impact of environmental exposures on ovarian function and role of xenobiotic metabolism during ovotoxicity. *Toxicol Appl Pharmacol* 2012; **261**:227–235.
13. Bhattacharya P, Keating AF. Ovarian metabolism of xenobiotics. *Exp Biol Med (Maywood)* 2011; **236**:765–771.
14. Borman SM, Christian PJ, Sipes IG, Hoyer PB. Ovotoxicity in female fischer rats and B6 mice induced by low-dose exposure to three polycyclic aromatic hydrocarbons: comparison through calculation of an ovotoxic index. *Toxicol Appl Pharmacol* 2000; **167**:191–198.
15. Keating AF, Sen N, Sipes IG, Hoyer PB. Dual protective role for glutathione S-transferase class pi against VCD-induced ovotoxicity in the rat ovary. *Toxicol Appl Pharmacol* 2010; **247**:71–75.
16. Hoyer PB. Can the clock be turned back on ovarian aging? *Sci Aging Knowledge Environ* 2004; **2004**:pe11.
17. Petrillo SK, Desmeules P, Truong TQ, Devine PJ. Detection of DNA damage in oocytes of small ovarian follicles following phosphoramide mustard exposures of cultured rodent ovaries in vitro. *Toxicol Appl Pharmacol* 2011; **253**:94–102.
18. Keating AF, J Mark C, Sen N, Sipes IG, Hoyer PB. Effect of phosphatidylinositol-3 kinase inhibition on ovotoxicity caused by 4-vinylcyclohexene diepoxide and 7, 12-dimethylbenz[a]anthracene in neonatal rat ovaries. *Toxicol Appl Pharmacol* 2009; **241**:127–134.
19. Cannady EA, Dyer CA, Christian PJ, Sipes IG, Hoyer PB. Expression and activity of cytochromes P450 2E1, 2A, and 2B in the mouse ovary: the effect of 4-vinylcyclohexene and its diepoxide metabolite. *Toxicol Sci* 2003; **73**:423–430.
20. Rajapaksa KS, Cannady EA, Sipes IG, Hoyer PB. Involvement of CYP 2E1 enzyme in ovotoxicity caused by 4-vinylcyclohexene and its metabolites. *Toxicol Appl Pharmacol* 2007; **221**:215–221.
21. Keating AF, Rajapaksa KS, Sipes IG, Hoyer PB. Effect of CYP2E1 gene deletion in mice on expression of microsomal epoxide hydrolase in response to VCD exposure. *Toxicol Sci* 2008; **105**:351–359.
22. Cannady EA, Dyer CA, Christian PJ, Sipes IG, Hoyer PB. Expression and activity of microsomal epoxide hydrolase in follicles isolated from mouse ovaries. *Toxicol Sci* 2002; **68**:24–31.
23. Igawa Y, Keating AF, Rajapaksa KS, Sipes IG, Hoyer PB. Evaluation of ovotoxicity induced by 7, 12-dimethylbenz[a]anthracene and its 3,4-diol metabolite utilizing a rat in vitro ovarian culture system. *Toxicol Appl Pharmacol* 2009; **234**:361–369.
24. Bhattacharya P, Keating AF. Protective role for ovarian glutathione S-transferase isoform pi during 7,12-dimethylbenz[a]anthracene-induced ovotoxicity. *Toxicol Appl Pharmacol* 2012; **260**:201–208.
25. Bhattacharya P, Madden JA, Sen N, Hoyer PB, Keating AF. Glutathione S-transferase class mu regulation of apoptosis signal-related kinase 1 protein during VCD-induced ovotoxicity in neonatal rat ovaries. *Toxicol Appl Pharmacol* 2012; **267**:49–56.
26. Hoyer PB, Sipes IG. Assessment of follicle destruction in chemical-induced ovarian toxicity. *Annu Rev Pharmacol Toxicol* 1996; **36**:307–331.
27. Hoyer PB. Damage to ovarian development and function. *Cell Tissue Res* 2005; **322**:99–106.
28. John GB, Gallardo TD, Shirley LJ, Castrillon DH. Foxo3 is a PI3K-dependent molecular switch controlling the initiation of oocyte growth. *Dev Biol* 2008; **321**:197–204.
29. Reddy P, Liu L, Adhikari D, Jagarlamudi K, Rajareddy S, Shen Y, Du C, Tang W, Hämäläinen T, Peng SL, Lan ZJ, Cooney AJ et al. Oocyte-specific deletion of Pten causes premature activation of the primordial follicle pool. *Science* 2008; **319**:611–613.
30. Reddy P, Zheng W, Liu K. Mechanisms maintaining the dormancy and survival of mammalian primordial follicles. *Trends Endocrinol Metab* 2010; **21**:96–103.
31. McGee EA, Hsueh AJ. Initial and cyclic recruitment of ovarian follicles. *Endocr Rev* 2000; **21**:200–214.
32. Chen Y-J, Hsiao P-W, Lee M-T, Mason JI, Ke F-C, Hwang J-J. Interplay of PI3K and cAMP/PKA signaling, and rapamycin-hypersensitivity in TGF beta 1 enhancement of FSH-stimulated steroidogenesis in rat ovarian granulosa cells. *J Endocrinol* 2007; **192**:405–419.
33. McDonald CA, Millena AC, Reddy S, Finlay S, Vizcarra J, Khan SA, Davis JS. Follicle-stimulating hormone-induced aromatase in immature rat sertoli cells requires an active phosphatidylinositol 3-kinase pathway and is inhibited via the mitogen-activated protein kinase signaling pathway. *Mol Endocrinol* 2006; **20**:608–618.
34. Zeleznik AJ, Saxena D, Little-Ihrig L. Protein kinase B is obligatory for follicle-stimulating hormone-induced granulosa cell differentiation. *Endocrinology* 2003; **144**:3985–3994.
35. Liu Z, Rudd MD, Hernandez-Gonzalez I, Gonzalez-Robayna I, Fan HY, Zeleznik AJ, Richards JS. FSH and FOXO1 regulate genes in the sterol/steroid and lipid biosynthetic pathways in granulosa cells. *Mol Endocrinol* 2009; **23**:649–661.
36. Nteeba J, Ross JW, Perfield Ii JW, Keating AF. High fat diet induced obesity alters ovarian phosphatidylinositol-3 kinase signaling gene expression. *Reprod Toxicol* 2013; **42**:68–77.
37. Martinez MN, Emfinger CH, Overton M, Hill S, Ramaswamy TS, Cappel DA, Wu K, Fazio S, McDonald WH, Hachey DL, Tabb DL, Stafford JM. Obesity and altered glucose metabolism impact HDL composition in CETP transgenic mice: a role for ovarian hormones. *J Lipid Res* 2012; **53**:379–389.
38. Wu S, Divall S, Wondisford F, Wolfe A. Reproductive tissues maintain insulin sensitivity in diet-induced obesity. *Diabetes* 2012; **61**:114–123.
39. Akamine EH, Marcal AC, Camporez JP, Hoshida MS, Caperuto LC, Bevilacqua E, Carvalho CR. Obesity induced by high-fat diet promotes insulin resistance in the ovary. *J Endocrinol* 2010; **206**:65–74.
40. Wang N, Luo LL, Xu JJ, Xu MY, Zhang XM, Zhou XL, Liu WJ, Fu YC. Obesity accelerates ovarian follicle development and follicle loss in rats. *Metabolism* 2014; **63**:94–103.
41. Acosta-Martinez M. PI3K: an attractive candidate for the central integration of metabolism and reproduction. *Front Endocrinol (Lausanne)* 2011; **2**:110.
42. Keating AF, Fernandez SM, Mark-Kappeler CJ, Sen N, Sipes IG, Hoyer PB. Inhibition of PIK3 signaling pathway members by the ovotoxicant 4-vinylcyclohexene diepoxide in rats. *Biol Reprod* 2011; **84**:743–751.
43. Bhattacharya P, Sen N, Hoyer PB, Keating AF. Ovarian expressed microsomal epoxide hydrolase: role in detoxification of 4-vinylcyclohexene diepoxide and regulation by phosphatidylinositol-3 kinase signaling. *Toxicol Appl Pharmacol* 2012; **258**:118–123.
44. Hoyer PB. Reproductive toxicology: current and future directions. *Biochem Pharmacol* 2001; **62**:1557–1564.
45. Nteeba J, Ganesan S, Keating AF. Progressive obesity alters ovarian folliculogenesis with impacts on pro-inflammatory and steroidogenic signaling in female mice. *Biol Reprod* 2014; **91**:86.
46. Klebig ML, Wilkinson JE, Geisler JG, Woychik RP. Ectopic expression of the agouti gene in transgenic mice causes obesity, features of type II diabetes, and yellow fur. *Proc Natl Acad Sci USA* 1995; **92**: 4728–4732.
47. Yang Z, Norwood KA, Smith JE, Kerl JG, Wood JR. Genes involved in the immediate early response and epithelial-mesenchymal transition

are regulated by adipocytokines in the female reproductive tract. *Mol Reprod Dev* 2012; **79**:128–137.
48. Carroll L, Voisey J, van Daal A. Mouse models of obesity. *Clin Dermatol* 2004; **22**:345–349.
49. Plowchalk DR, Mattison DR. Phosphoramide mustard is responsible for the ovarian toxicity of cyclophosphamide. *Toxicol Appl Pharmacol* 1991; **107**:472–481.
50. Nteeba J, Ganesan S, Keating AF. Impact of obesity on ovotoxicity induced by 7,12-dimethylbenz[a]anthracene in mice. *Biol Reprod* 2014; **90**:68.
51. Owens LA, Avalos G, Kirwan B, Carmody L, Dunne F. ATLANTIC DIP: closing the loop: a change in clinical practice can improve outcomes for women with pregestational diabetes. *Diabetes Care* 2012; **35**:1669–1671.
52. Purcell SH, Moley KH. The impact of obesity on egg quality. *J Assist Reprod Genet* 2011; **28**:517–524.
53. Brown C, LaRocca J, Pietruska J, Ota M, Anderson L, Smith SD, Weston P, Rasoulpour T, Hixon ML. Subfertility caused by altered follicular development and oocyte growth in female mice lacking PKB alpha/Akt1. *Biol Reprod* 2010; **82**:246–256.
54. Liu L, Rajareddy S, Reddy P, Jagarlamudi K, Du C, Shen Y, Guo Y, Boman K, Lundin E, Ottander U, Selstam G, Liu K. Phosphorylation and inactivation of glycogen synthase kinase-3 by soluble kit ligand in mouse oocytes during early follicular development. *J Mol Endocrinol* 2007; **38**:137–146.
55. Reddy P, Adhikari D, Zheng W, Liang S, Hamalainen T, Tohonen V, Ogawa W, Noda T, Volarevic S, Huhtaniemi I, Liu K. PDK1 signaling in oocytes controls reproductive aging and lifespan by manipulating the survival of primordial follicles. *Hum Mol Genet* 2009; **18**:2813–2824.
56. Rajareddy S, Reddy P, Du C, Liu L, Jagarlamudi K, Tang W, Shen Y, Berthet C, Peng SL, Kaldis P, Liu K. p27kip1 (cyclin-dependent kinase inhibitor 1B) controls ovarian development by suppressing follicle endowment and activation and promoting follicle atresia in mice. *Mol Endocrinol* 2007; **21**:2189–2202.
57. Jagarlamudi K, Liu L, Adhikari D, Reddy P, Idahl A, Ottander U, Lundin E, Liu K. Oocyte-specific deletion of Pten in mice reveals a stage-specific function of PTEN/PI3K signaling in oocytes in controlling follicular activation. *PLoS One* 2009; **4**:e6186.
58. Reddy P, Liu L, Adhikari D, Jagarlamudi K, Rajareddy S, Shen Y, Du C, Tang W, Hamalainen T, Peng SL, Lan ZJ, Cooney AJ et al. Oocyte-specific deletion of Pten causes premature activation of the primordial follicle pool. *Science* 2008; **319**:611–613.
59. Liu L, Rajareddy S, Reddy P, Du C, Jagarlamudi K, Shen Y, Gunnarsson D, Selstam G, Boman K, Liu K. Infertility caused by retardation of follicular development in mice with oocyte-specific expression of Foxo3a. *Development* 2007; **134**:199–209.
60. Zhang Y, Proenca M, Maffei M, Barrone M, Leopold L, Friedman J. Positional cloning of the mouse obese gene and its human homologue. *Nature* 1994; **372**:425–432.
61. Tartaglia L, Dembski M, Weng X, Deng N, Culpepper J, Devos R, Richards G, Campfield L, Clark F, Deeds J. Identification and expression cloning of a leptin receptor, OB-R. *Cell* 1995; **83**:1263–1271.
62. Brannian J, Eyster K, Greenway M, Henriksen C, Teslaa K, Diggins M. Progressive obesity leads to altered ovarian gene expression in the Lethal Yellow mouse: a microarray study. *J Ovarian Res* 2009; **2**:10.
63. Duhl DM, Stevens ME, Vrieling H, Saxon PJ, Miller MW, Epstein CJ, Barsh GS. Pleiotropic effects of the mouse lethal yellow (Ay) mutation explained by deletion of a maternally expressed gene and the simultaneous production of agouti fusion RNAs. *Development* 1994; **120**:1695–1708.
64. Michaud EJ, Bultman SJ, Klebig ML, van Vugt MJ, Stubbs LJ, Russell LB, Woychik RP. A molecular model for the genetic and phenotypic characteristics of the mouse lethal yellow (Ay) mutation. *Proc Natl Acad Sci USA* 1994; **91**:2562–2566.
65. Lu D, Willard D, Patel I, Kadwell S, Overton L, Kost T, Luther M, Chen W, Woychik R, Wilkison W. Agouti protein is an antagonist of the melanocyte-stimulating hormone receptor. *Nature* 1994; **371**:799–802.
66. Bray GA. Obesity and reproduction. *Human Reprod* 1997; **12**:26–32.
67. Brannian J, Furman G, Diggins M. Declining fertility in the Lethal Yellow mouse is related to progressive hyperleptinemia and leptin resistance. *Reprod Nutr Dev* 2005; **45**:143–150.
68. Halaas J, Boozer C, Blair-West J, Fidahusein N, Denton D, Friedman J. Physiological response to long-term peripheral and central leptin infusion in lean and obese mice. *Proc Natl Acad Sci USA* 1997; **94**:8878–8883.
69. Granholm N, Jeppesen K, Japs R. Progressive infertility in female lethal yellow mice (Ay/a; strain C57BL/6J). *J Reprod Fertil* 1986; **76**:279–287.
70. Hogan C, Sehr H, Diggins M. Premature lengthening and cessation of estrous cycles in the lethal yellow mouse. *Proc SD Acad Sci* 1991; **70**:249.
71. Valckx SDM, De Pauw I, De Neubourg D, Inion I, Berth M, Fransen E, Bols PEJ, Leroy JLMR. BMI-related metabolic composition of the follicular fluid of women undergoing assisted reproductive treatment and the consequences for oocyte and embryo quality. *Human Reprod* 2012; **27**:3531–3539.
72. Robker RL, Akison LK, Bennett BD, Thrupp PN, Chura LR, Russell DL, Lane M, Norman RJ. Obese women exhibit differences in ovarian metabolites, hormones, and gene expression compared with moderate-weight women. *J Clin Endocrinol Metab* 2009; **94**:1533–1540.
73. Brothers KJ, Wu S, DiVall SA, Messmer MR, Kahn CR, Miller RS, Radovick S, Wondisford FE, Wolfe A. Rescue of obesity-induced infertility in female mice due to a pituitary-specific knockout of the insulin receptor. *Cell Metab* 2010; **12**:295–305.
74. Sun XJ, Miralpeix M, Myers MG, Jr, Glasheen EM, Backer JM, Kahn CR, White MF. Expression and function of IRS-1 in insulin signal transmission. *J Biol Chem* 1992; **267**:22662–22672.
75. Myers MG, Jr, Sun XJ, Cheatham B, Jachna BR, Glasheen EM, Backer JM, White MF. IRS-1 is a common element in insulin and insulin-like growth factor-I signaling to the phosphatidylinositol 3'-kinase. *Endocrinology* 1993; **132**:1421–1430.
76. Gual P, Le Marchand-Brustel Y, Tanti JF. Positive and negative regulation of insulin signaling through IRS-1 phosphorylation. *Biochimie* 2005; **87**:99–109.
77. Giraud J, Leshan R, Lee Y-H, White MF. Nutrient-dependent and insulin-stimulated phosphorylation of insulin receptor substrate-1 on serine 302 correlates with increased insulin signaling. *J Biol Chem* 2004; **279**:3447–3454.
78. Danielsson A, Öst A, Nystrom FH, Strålfors P. Attenuation of insulin-stimulated insulin receptor substrate-1 serine 307 phosphorylation in insulin resistance of type 2 diabetes. *J Biol Chem* 2005; **280**:34389–34392.
79. Öst A, Danielsson A, Lidén M, Eriksson U, Nystrom FH, Strålfors P. Retinol-binding protein-4 attenuates insulin-induced phosphorylation of IRS1 and ERK1/2 in primary human adipocytes. *FASEB J* 2007; **21**:3696–3704.
80. Weigert C, Kron M, Kalbacher H, Pohl AK, Runge H, Häring H-U, Schleicher E, Lehmann R. Interplay and effects of temporal changes in the phosphorylation state of serine-302, -307, and -318 of insulin receptor substrate-1 on insulin action in skeletal muscle cells. *Mol Endocrinol* 2008; **22**:2729–2740.
81. Hirosumi J, Tuncman G, Chang L, Gorgun CZ, Uysal KT, Maeda K, Karin M, Hotamisligil GS. A central role for JNK in obesity and insulin resistance. *Nature* 2002; **420**:333–336.
82. Werner ED, Lee J, Hansen L, Yuan M, Shoelson SE. Insulin resistance due to phosphorylation of insulin receptor substrate-1 at serine 302. *J Biol Chem* 2004; **279**:35298–35305.
83. Rui L, Aguirre V, Kim JK, Shulman GI, Lee A, Corbould A, Dunaif A, White MF. Insulin/IGF-1 and TNF-alpha stimulate phosphorylation of IRS-1 at inhibitory Ser307 via distinct pathways. *J Clin Invest* 2001; **107**:181–189.
84. Louhio H, Hovatta O, Sjoberg J, Tuuri T. The effects of insulin, and insulin-like growth factors I and II on human ovarian follicles in long-term culture. *Mol Hum Reprod* 2000; **6**:694–698.
85. Serafim MKB, Silva GM, Duarte ABG, Araújo VR, Silva TFP, Lima AKF, Chaves RN, Campello CC, Silva LDM, Figueiredo JR. High insulin

concentrations promote the in vitro growth and viability of canine preantral follicles. *Reprod Fertil Dev* 2013; **25**:927–934.
86. Yu N, Roy SK. Development of primordial and prenatal follicles from undifferentiated somatic cells and oocytes in the hamster prenatal ovary in vitro: effect of insulin. *Biol Reprod* 1999; **61**:1558–1567.
87. Kezele PR, Nilsson EE, Skinner MK. Insulin but not insulin-like growth factor-1 promotes the primordial to primary follicle transition. *Mol Cell Endocrinol* 2002; **192**:37–43.
88. Fortune JE. The early stages of follicular development: activation of primordial follicles and growth of preantral follicles. *Anim Reprod Sci* 2003; **78**:135–163.
89. Nilsson EE, Kezele P, Skinner MK. Leukemia inhibitory factor (LIF) promotes the primordial to primary follicle transition in rat ovaries. *Mol Cell Endocrinol* 2002; **188**:65–73.
90. Kim YB, Peroni OD, Franke TF, Kahn BB. Divergent regulation of Akt1 and Akt2 isoforms in insulin target tissues of obese Zucker rats. *Diabetes* 2000; **49**:847–856.
91. Vincent EE, Elder DJ, Thomas EC, Phillips L, Morgan C, Pawade J, Sohail M, May MT, Hetzel MR, Tavare JM. Akt phosphorylation on Thr308 but not on Ser473 correlates with Akt protein kinase activity in human non-small cell lung cancer. *Br J Cancer* 2011; **104**:1755–1761.
92. Blume-Jensen P, Hunter T. Oncogenic kinase signalling. *Nature* 2001; **411**:355–365.
93. Toker A, Newton AC. Cellular signaling: pivoting around PDK-1. *Cell* 2000; **103**:185–188.
94. Dong XC, Copps KD, Guo S, Li Y, Kollipara R, DePinho RA, White MF. Inactivation of hepatic Foxo1 by insulin signaling is required for adaptive nutrient homeostasis and endocrine growth regulation. *Cell Metab* 2008; **8**:65–76.
95. Long YC, Cheng Z, Copps KD, White MF. Insulin receptor substrates Irs1 and Irs2 coordinate skeletal muscle growth and metabolism via the Akt and AMPK pathways. *Mol Cell Biol* 2011; **31**:430–441.
96. Cho H, Mu J, Kim JK, Thorvaldsen JL, Chu Q, Crenshaw EB, 3rd, Kaestner KH, Bartolomei MS, Shulman GI, Birnbaum MJ. Insulin resistance and a diabetes mellitus-like syndrome in mice lacking the protein kinase Akt2 (PKB beta). *Science* 2001; **292**:1728–1731.
97. Copps KD, White MF. Regulation of insulin sensitivity by serine/threonine phosphorylation of insulin receptor substrate proteins IRS1 and IRS2. *Diabetologia* 2012; **55**:2565–2582.
98. Reddy P, Shen L, Ren C, Boman K, Lundin E, Ottander U, Lindgren P, Liu YX, Sun QY, Liu K. Activation of Akt (PKB) and suppression of FKHRL1 in mouse and rat oocytes by stem cell factor during follicular activation and development. *Dev Biol* 2005; **281**:160–170.
99. Arden KC, Biggs WH, 3rd. Regulation of the FoxO family of transcription factors by phosphatidylinositol-3 kinase-activated signaling. *Arch Biochem Biophys* 2002; **403**:292–298.
100. Castrillon DH, Miao L, Kollipara R, Horner JW, DePinho RA. Suppression of ovarian follicle activation in mice by the transcription factor Foxo3a. *Science* 2003; **301**:215–218.
101. Liu K, Rajareddy S, Liu L, Jagarlamudi K, Boman K, Selstam G, Reddy P. Control of mammalian oocyte growth and early follicular development by the oocyte PI3 kinase pathway: new roles for an old timer. *Dev Biol* 2006; **299**:1–11.
102. Liu K. Stem cell factor (SCF)-kit mediated phosphatidylinositol 3 (PI3) kinase signaling during mammalian oocyte growth and early follicular development. *Front Biosci* 2006; **11**:126–135.
103. Kissel H, Timokhina I, Hardy MP, Rothschild G, Tajima Y, Soares V, Angeles M, Whitlow SR, Manova K, Besmer P. Point mutation in kit receptor tyrosine kinase reveals essential roles for kit signaling in spermatogenesis and oogenesis without affecting other kit responses. *EMBO J* 2000; **19**:1312–1326.
104. Horie K, Takakura K, Taii S, Narimoto K, Noda Y, Nishikawa S, Nakayama H, Fujita J, Mori T. The expression of c-kit protein during oogenesis and early embryonic development. *Biol Reprod* 1991; **45**:547–552.
105. Manova K, Nocka K, Besmer P, Bachvarova RF. Gonadal expression of c-kit encoded at the W locus of the mouse. *Development* 1990; **110**:1057–1069.
106. Manova K, Huang EJ, Angeles M, De Leon V, Sanchez S, Pronovost SM, Besmer P, Bachvarova RF. The expression pattern of the c-kit ligand in gonads of mice supports a role for the c-kit receptor in oocyte growth and in proliferation of spermatogonia. *Dev Biol* 1993; **157**:85–99.
107. Driancourt MA, Reynaud K, Cortvrindt R, Smitz J. Roles of KIT and KIT LIGAND in ovarian function. *Rev Reprod* 2000; **5**:143–152.
108. Ismail RS, Okawara Y, Fryer JN, Vanderhyden BC. Hormonal regulation of the ligand for c-kit in the rat ovary and its effects on spontaneous oocyte meiotic maturation. *Mol Reprod Dev* 1996; **43**:458–469.
109. Palma GA, Arganaraz ME, Barrera AD, Rodler D, Mutto AA, Sinowatz F. Biology and biotechnology of follicle development. *ScientificWorldJournal* 2012; **2012**:938138.
110. Parrott JA, Skinner MK. Kit-ligand/stem cell factor induces primordial follicle development and initiates folliculogenesis. *Endocrinology* 1999; **140**:4262–4271.
111. Parrott JA, Skinner MK. Kit ligand actions on ovarian stromal cells: effects on theca cell recruitment and steroid production. *Mol Reprod Dev* 2000; **55**:55–64.
112. Yoshida H, Takakura N, Kataoka H, Kunisada T, Okamura H, Nishikawa SI. Stepwise requirement of c-kit tyrosine kinase in mouse ovarian follicle development. *Dev Biol* 1997; **184**:122–137.
113. Packer AI, Hsu YC, Besmer P, Bachvarova RF. The ligand of the c-kit receptor promotes oocyte growth. *Dev Biol* 1994; **161**:194–205.
114. Fortune JE, Yang MY, Muruvi W. The earliest stages of follicular development: follicle formation and activation. *Soc Reprod Fertil Suppl* 2010; **67**:203–216.
115. Miyoshi T, Otsuka F, Nakamura E, Inagaki K, Ogura-Ochi K, Tsukamoto N, Takeda M, Makino H. Regulatory role of kit ligand–c-kit interaction and oocyte factors in steroidogenesis by rat granulosa cells. *Mol Cell Endocrinol* 2012; **358**:18–26.
116. Carlsson IB, Laitinen MP, Scott JE, Louhio H, Velentzis L, Tuuri T, Aaltonen J, Ritvos O, Winston RM, Hovatta O. Kit ligand and c-Kit are expressed during early human ovarian follicular development and their interaction is required for the survival of follicles in long-term culture. *Reproduction* 2006; **131**:641–649.
117. Woodcroft KJ, Novak RF. The role of phosphatidylinositol 3-kinase, Src kinase, and protein kinase A signaling pathways in insulin and glucagon regulation of CYP2E1 expression. *Biochem Biophys Res Commun* 1999; **266**:304–307.
118. Woodcroft KJ, Hafner MS, Novak RF. Insulin signaling in the transcriptional and posttranscriptional regulation of CYP2E1 expression. *Hepatology* 2002; **35**:263–273.
119. Bellward GD, Chang T, Rodrigues B, McNeill JH, Maines S, Ryan DE, Levin W, Thomas PE. Hepatic cytochrome P-450j induction in the spontaneously diabetic BB rat. *Mol Pharmacol* 1988; **33**:140–143.
120. Gonzalez FJ. CYP2E1. *Drug Metab Disp* 2007; **35**:1–8.
121. Song BJ, Veech RL, Saenger P. Cytochrome P450IIE1 is elevated in lymphocytes from poorly controlled insulin-dependent diabetics. *J Clin Endocrinol Metab* 1990; **71**:1036–1040.
122. Kim SK, Novak RF. The role of intracellular signaling in insulin-mediated regulation of drug metabolizing enzyme gene and protein expression. *Pharmacol Ther* 2007; **113**:88–120.
123. Kim SK, Woodcroft KJ, Kim SG, Novak RF. Insulin and glucagon signaling in regulation of microsomal epoxide hydrolase expression in primary cultured rat hepatocytes. *Drug Metab Dispos* 2003; **31**:1260–1268.
124. Thomas H, Schladt L, Knehr M, Oesch F. Effect of diabetes and starvation on the activity of rat liver epoxide hydrolases, glutathione S-transferases and peroxisomal beta-oxidation. *Biochem Pharmacol* 1989; **38**:4291–4297.
125. Franco R, Schoneveld OJ, Pappa A, Panayiotidis MI. The central role of glutathione in the pathophysiology of human diseases. *Arch Physiol Biochem* 2007; **113**:234–258.
126. Ki SH, Kim SG. Phase II enzyme induction by alpha-lipoic acid through phosphatidylinositol 3-kinase-dependent C/EBPs activation. *Xenobiotica* 2008; **38**:587–604.
127. Listowsky I, Abramovitz M, Homma H, Niitsu Y. Intracellular binding and transport of hormones and xenobiotics by glutathione-S-transferases. *Drug Metab Rev* 1988; **19**:305–318.

128. Henderson CJ, Smith AG, Ure J, Brown K, Bacon EJ, Wolf CR. Increased skin tumorigenesis in mice lacking pi class glutathione S-transferases. *Proc Natl Acad Sci USA* 1998; **95**:5275–5280.
129. Green JA, Robertson LJ, Clark AH. Glutathione S-transferase expression in benign and malignant ovarian tumours. *Br J Cancer* 1993; **68**:235–239.
130. Hayes JD, Pulford DJ. The glutathione S-transferase supergene family: regulation of GST and the contribution of the isoenzymes to cancer chemoprotection and drug resistance. *Crit Rev Biochem Mol Biol* 1995; **30**:445–600.
131. Townsend D, Tew K. Cancer drugs, genetic variation and the glutathione-S-transferase gene family. *Am J Pharmacogenomics* 2003; **3**:157–172.
132. Townsend DM, Tew KD. The role of glutathione-S-transferase in anti-cancer drug resistance. *Oncogene* 2003; **22**:7369–7375.
133. Tew KD, Townsend DM. Regulatory functions of glutathione S-transferase P1-1 unrelated to detoxification. *Drug Metab Rev* 2011; **43**:179–193.
134. Tew KD. Drug resistance in cancer. Editorial. *Biochem Pharmacol* 2012; **83**:985–986.
135. Morrow CS, Diah S, Smitherman PK, Schneider E, Townsend AJ. Multidrug resistance protein and glutathione S-transferase P1-1 act in synergy to confer protection from 4-nitroquinoline 1-oxide toxicity. *Carcinogenesis* 1998; **19**:109–115.
136. Ganesan S, Nteeba J, Madden JA, Keating AF. Obesity alters phosphoramide mustard-induced ovarian DNA repair. *Biol Reprod* Under Review.
137. Madden JA, Keating AF. Ovarian xenobiotic biotransformation enzymes are altered during phosphoramide mustard-induced ovotoxicity. *Toxicol Sci* 2014; **141**:441–452.
138. Madden JA, Hoyer PB, Devine PJ, Keating AF. Involvement of a volatile metabolite during phosphoramide mustard-induced ovotoxicity. *Toxicol Appl Pharmacol* 2014; **277**:1–7.
139. Rauen HM, Norpoth K. A volatile alkylating agent in the exhaled air following the administration of Endoxan. *Klin Wochenschr* 1968; **46**:272–275.